NUMERICAL SIMULATION FOR SEAWATER AIR PRECOOLER

H.A. Etaiwe*[1], R.Y. Sakr[1], M. R. Salem[1], H.E. Abdelrahman[1]

[1] Mechanical Engineering Department, Faculty of Engineering at Shoubra, Benha University, Cairo, Egypt

Corresponding: **Husain965@yahoo.com**

ABSTRACT

The low-temperature seawater is an important renewable source used for direct and indirect seawater air conditioning. In the northern Arabian Gulf, the water depth is insufficient for direct seawater air conditioning. So, for such circumstances, seawater can be utilized as an auxiliary for precooling the returned air from the conditioned space. In this study, a two-dimensional numerical simulation model of crossflow for a 20-tube bank in a staggered arrangement with a diameter of 25 mm was investigated, with the pitch ratio S_L/D and S_T/D as 1.5 and 1.25 respectively. The air inlet velocity ranged from 2 to 5 m/s, the air inlet temperature is 28°C, and the seawater temperature of 21°C was considered.

This paper summarized the numerical study to predict the performance of a heat exchanger an as air precooler by utilizing the seawater as a cold stream. The effect of tube bank arrangement is also investigated. ANSYS 20 was applied for the numerical simulation, and the best results obtained of the temperature after the air precooling coil is 22.75°C that resulting in the efficiency of the air conditioning system maximum improvement by 37.5 %.

المحاكاة العدديه لاستخدام ماء البحر لتبريد الهواء الابتدائي

حسين علي عتيوي`، رمضان يوسف صقر`، محمد رضا سالم` ، هاني عبد الرحمن الصاوي`

قسم الهندسه الميكانيكيه، كلية هندسة شبرا، جامعة بنها، القاهره ، مصر

اميل الباحث الرئيسي: Husain965@yahoo.com

الملخص

ماء البحر بدرجة حراره منخفضه مصدر مهم للطاقه النظيفه يمكن استخدامه لتكييف الهواء المباشر وغير المباشر. في شمال الخليج العربي درجة حرارة ماء البحر غير كافيه لهذا الغرض كون الأعماق ضحله لذا ممكن الاستفاده منها في التبريد الابتدائي. في هذه الدراسه تم دراسة مقاطع طوليه لنماذج ثنائية الابعاد لحزمة انابيب مكونه أكثر من ٢٠ أنبوب بأقطار ٢٥ ملم مرتبه على

شكل خطي وثلاثي، نسبة الخطوه الطوليه والعرضيه الى القطر هي ١,٥ و١,٢٥، سرعة دخول الهواء بين ٢ الى ٥ م/ثا، درجة حرارة الهواء الداخل للمبادل الحراري هي ٢٨ م° ودرجة حرارة ماء البحر هي ٢١ م° استخدمت معطيات لتشغيل البرنامج، تم اختيار النموذج ٢٠ أنبوب ثنائي الترتيب لأفضلية النتائج.
استخدم برنامج ANSYS20 مع ديناميك السوائل الحسابيه CFD لحل معادلات الكتله والزخم والطاقه والسرعه , أظهرت النتائج الحصول على درجات حراره بعد المبادل ٢٢,٧٥ م وهذا مما يزيد من كفاءة منظومة التبريد بنسبة ٣٧,٥٪.

1. Introduction

In industries, many applications are found for heat exchangers which deal with the heat exchanging between two fluids at different temperatures, such as air, water, oil, …, etc. The heat exchangers are classified according to the flow direction as parallel, counter, and cross flow patterns, most of the equipment use the cross flow pattern. The heat exchanger with tube banks is arranged into inline and staggered arrangements. There are many techniques to enhance the process of heat exchange. These techniques are divided into active types that influenced by external force or passive types without external effect depending on the geometry, material, size, and the load type for heat transfer. Researchers discussed the possibility of increasing the effectiveness of heat exchangers in various applications.

Lee et al [1], used a numerical model to show how longitudinal pitch changes affects the thermal performance of inline tube bank pattern. The overall heat transfer across the tube bank was compared to the correlation that already existed. The pitch ratio in each direction was confirmed to be a factor in the relationship. In addition, a general correlation for Nusselt number for each row was obtained. Xu et al. [2], numerically investigated the characteristics of the flow and the heat transfer for 6 rows finned tube bank of 3D aligned external rectangular. Their results were compared with a smooth tube bank and the effect of transverse, longitudinal, fin pitches in the axial direction as well as Reynolds number is analyzed. Three dimensional CFD model was developed by Lui et al. [3] by studying the effect of longitudinal and transverse pitch of heat recovery device used in wind tower system on the ventilation and thermal performance. Their results showed that the heat recovery was improved by reducing the pitches in the two directions raising the fresh air temperature up to 64°C. Souza, et al. [4] investigated numerically an evaporator for two-dimensional models of window air conditioner type. They used market available sizes copper pipes of six transverse pitch with velocity range 1.5 to 4 m/s. The effects of transverse pitches on the Nusselt number, heat transfer coefficient, pressure drop, and friction factor in a tube bank are illustrated. Their study proved the effects of transverse pitch on the heat transfer and velocity of flow at constant surface temperature, where the study recorded that when the pitch was lower the heat transfer was lower, and if the pitch increased the Nusselt number so increase with increasing the size of the tube. In the inline arrangement, tube performance becomes better for large diameters than for smaller ones.

Pelaez, et al. [5] showed that the air side Nusselt number and the friction factor are influenced by Reynolds number, fin pitch, tube diameter, and fin length and fin thickness in air water heat exchanger. The results from their model showed real temperature contours, due to the consideration of water flow in tubes and wall conduction. Medina et al. [6], introduced a new model for calculating heat transfer during airflow through finned tubes bank in air cooled condenser systems. The experiments were conducted for transverse and longitudinal pitches intervals range 0.4-2, air flow velocity of 0.1 to 100 m/s, an ambient temperature of 15 to 43°C, the outer equivalent diameter of the bare tubes between 0.019 and 0.05 m, a fins height range 2.7-7.9 mm. The fins thicknesses ranging between 1.3 and 3.5 mm and the number of fins per unit tube length ranges 315-394. In 85.3% of the experimental data that were correlated, the mean deviation was 6.9%. Using the generalized pattern search technique, researchers studied numerical optimization (GPSA). By employing an entropy minimization technique, Khan et al. [7] investigated the thermodynamic losses brought by the fluid pressure drop and heat transfer in cross flow across tube banks. A universal dimensionless equation was provided for the rate of entropy generation. Analytical/empirical correlations for heat transfer coefficient and friction factor are applied for both inline and staggered patterns. Sahamifar et al. [8], investigated the optimal longitudinal and transverse pitches of staggered tube banks in a turbulent flow regime. Without considering the overall volume, symmetric and periodic boundary conditions are employed to simulate all the tube banks. By simulating flow and heat transfer of bank tube by CFD, the optimization process can be carried out directly utilizing these boundary conditions; the correlations from earlier studies are not utilized in this procedure. As the goal function, the "goodness factor" is used, which considers the impacts of both heat transfer and pressure drop in the right sequence. In the first section of the investigation, the best pitches are predicted for inlet Reynolds and Prandtl values. The impact of inlet Reynolds and Prandtl numbers on the appropriate pitches in the turbulent flow is independently investigated. Using a computational fluid dynamic simulation software, Fluent 6.2, Abdel-Rehim [9] a computational analysis of heat transfer and turbulent fluid flow across a bank of circular tubes with staggered lengths was reported. The model for staggered configurations can be used over a wide range of aspect ratios. The results show that aspect ratio, Reynolds number, and Prandtl number, in the cross flow pattern over bank tube effected on the heat transfer. Often, near the initial of the exterior tube, the higher pressure drop distribution values are always found. In the space between the upper and lower sides, the greatest velocity was found. The average Nusselt numbers with Reynolds number obtained here at an aspect ratio of 1.5 are in good match with previous data published. Mangrulkar et al. [10], conducted an experimental analysis and 3D simulation of air cross flow over a staggered tube bank with and without a splitter plate attached to the tube for Reynolds numbers ranging from 5500 to 14500. The ratio of length to the diameter is one, and the longitudinal and transverse tube pitch ratios were set to 1.75 and 2, respectively. Due to increased heat transfer and a decreased friction factor, the splitter plate attachment resulted in better overall thermal performance. At Re=5500, employing the splitter plate over the bare cylinders resulted in a maximum gain of 60-82 percent of thermal performance. El Mekawy et al. [11], developed a CFD model to simulate cross flow across a staggered circular tube bank inside a heat exchanger. They

demonstrated the impact of connecting the circular tubes with a splitter. Heat transfer is increased by 7% and pressure drop is increased by 20% when the splitter thickness is increased to 20% of the tube diameter. The heat transfer was doubled, and the pressure loss was increased by 20% when the splitter length ratio was increased to 1.5. The effect of a longitudinal taper fin on the external flow through a staggered tube bank was studied numerically by Abraham et al. [12]. The length to tube diameter ratio of the fins was 0.5 to 1.5, while the fin thickness to tube diameter ratio was 0.4 to 0.6. Their findings suggest that using longitudinal taper fins improves the thermal hydraulic performance of a cross flow over staggered tube bank greatly. Surroop and Abhishekanand [13], conducted a study to evaluate the technical and economic aspects of utilizing seawater for air conditioning for hotels near the sea with a cooling load more than 900 tonnes, or 3.5 GW. The conventional air conditioning system with a chiller (Option 1), air conditioning by direct seawater (Option 2), and seawater air conditioning system with chiller (Option 3) were chosen for research. The power consumption of each system to meet the hotel cooling load was the subject of the technical evaluation of the three solutions. The power usage for the three alternatives was found to be 3500 kW, 470 kW, and 1870 kW, respectively. When compared to option 1, the gases emissions that would be averted by implementing options 2 and 3 were found to be 13 tonne and 7 tonne per day, respectively. The present work aims to illustrate the best design for air precooler that utilizes the Arabian Gulf seawater where the depth is around 40 m to 60m for air precooling air conditioning system.

2. Description of the geometry

Figure (1) shows the proposed single stage LiBr-water absorption air conditioning system [16], that takes the benefit of the cold sea water from the shallow depth Arabian gulf to precool the mixed air before entering the cooling coil.
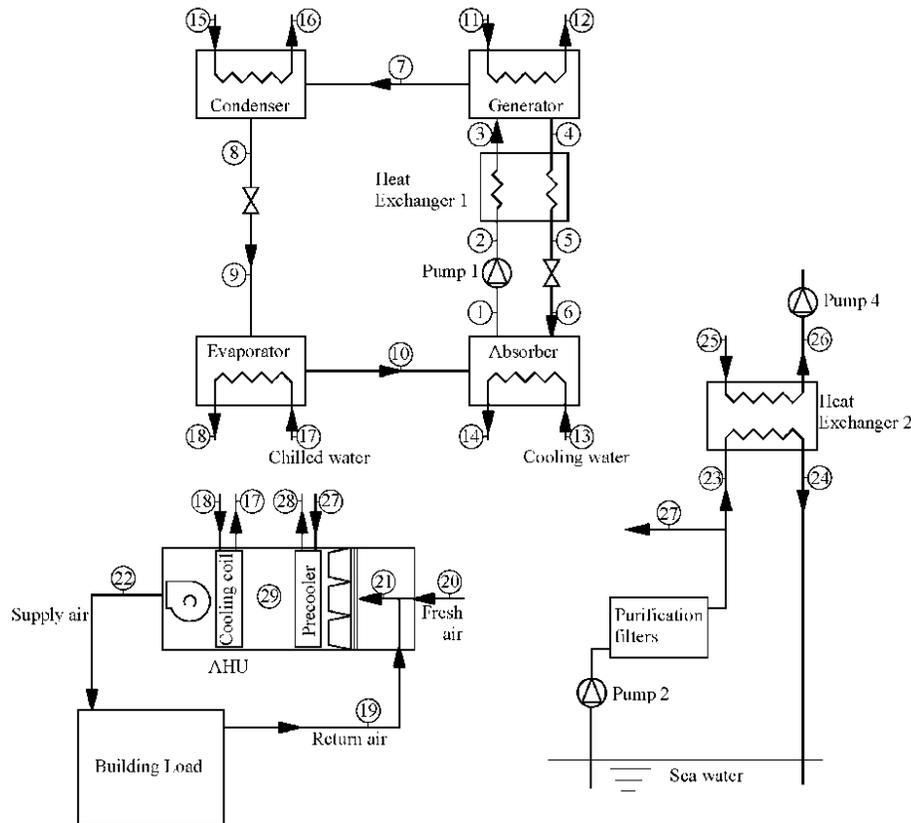
Fig. 1: Air- conditioning single effect LiBr-H2O absorption system using sea water for cooling the condenser and absorber with air precooling

2.1 The air precooling process

Figure 2 shows a longitudinal section domain of the model consisting of 20 tubes with dimensions of (525x62.5) mm in a staggered arrangement by 2*10 columns and rows. The model is chosen among several studied models as 30, 40, 50, 60, and 70 bank tubes due to the appropriate size and the results, the diameter of the tube is 25 mm where the dimensionless transverse and longitudinal pitches ratios, S_L/D=1.5, S_T/D =1.25 respectively. The material used for the heat exchanger is aluminum–titanium alloy to resist the corrosion caused by seawater.

In the current work, it is assumed that the mixed air with a temperature of 28°resulted from the mixing of the return air from the conditioned space with the fresh air from the outdoor. The air velocity inlet to the heat exchanger ranged from 2 to 5 m/s. Figure 2 shows the seawater withdrawn from the sea into tube a bank with a temperature of 21°C. The temperature of mixed air cooled down when passing over the tube surfaces of a seawater heat exchanger and further cooling of the air is achieved by the evaporator coil then supply the air to the conditioned space at 14°C. ANSYS 20 software has been used to perform the numerical simulation.

The maximum fluid velocity of air inside the tube bank depends on the throat area A_T and on the diagonal throat area A_D. the fluid flow across the tube bank is first passed through the throat area A_T then though $2A_D$. So, If $2A_D > A_T$ the maximum velocity across A_T is given as:

$$V_{max} = \frac{U. S_T}{(S_T - D)} \tag{1}$$

If $2A_D < A_T$

$$V_{max} = \frac{U.S_T}{2(S_T - D)} \tag{2}$$

The Reynolds number is given by:

$$Re = \frac{\rho.V_{max}.D}{\mu} \tag{3}$$

The tube heat transfer rate as:

$$Q = h . A (T_S - T_a) \tag{4}$$

So, the heat transfer coefficient is:

$$h = \frac{Q}{A(T_a - T_s)}$$

and Nusselt number as:

$$Nu = \frac{h.D}{K} \tag{5}$$

The friction as:

$$f = \frac{\Delta p . 2}{\rho(V_{max})^2} . \frac{A_{min}}{A_{max}} \tag{6}$$

where Δp is the pressure drop across the tube bank, A_{min} and A_{max} are the minimum and the maximum surface area of the tube bank.
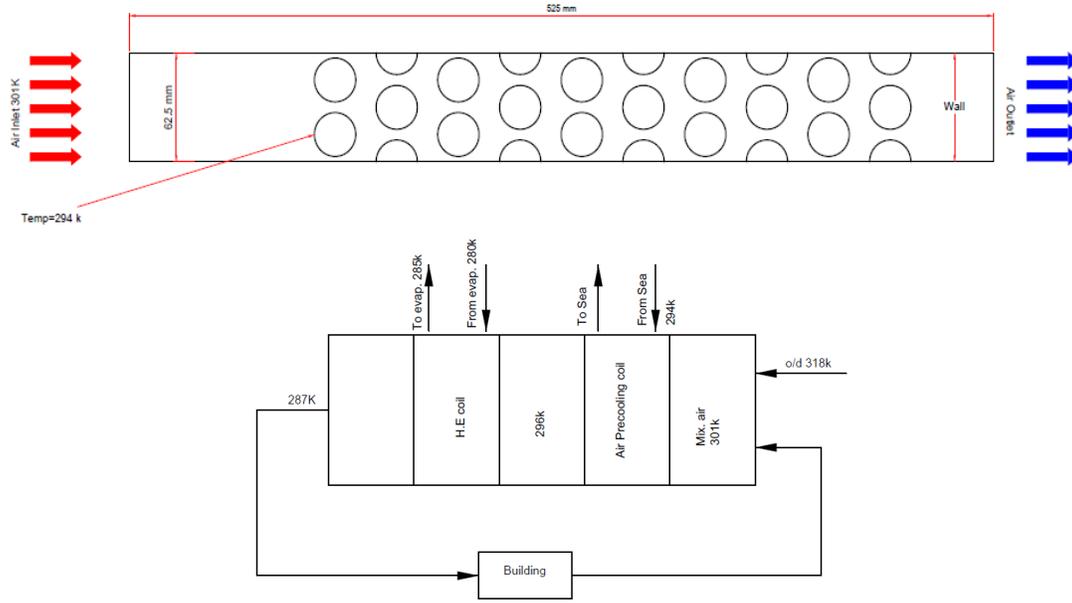
Fig. 2 Geometry domain and schematic of air precooling process

3. Mathematical Model and Numerical Simulation

The governing equations consider the fundamental mathematical equations for solving the fluid flow analysis. The flow is assumed to be incompressible, single-phase, fully devolved and steady. The turbulence model used in the current work is k-ε realizable.

Continuity equation

$$\frac{\partial(\rho u_j)}{\partial x_j} = 0 \tag{7}$$

Momentum conservation equation

$$\frac{\partial(\rho u_i u_j)}{\partial x_j} = -\frac{\partial p}{\partial x_i} + \frac{\partial}{\partial x_j}\left[\mu\left(\frac{\partial u_i}{\partial x_j} + \frac{\partial u_i}{\partial x_j}\right)\right] + \frac{\partial}{\partial x_j}\left(-\rho\overline{\acute{u}_i\acute{u}_j}\right) \tag{8}$$

Energy conservation equation:

$$\frac{\partial(\rho u_i T)}{\partial x_j} = \frac{\partial}{\partial x_j}\left(\frac{\mu}{Pr}\frac{\partial T}{\partial x_j} - \rho\overline{\acute{T}\acute{u}_j}\right) \tag{9}$$

The term $-\rho\overline{\acute{u}_i\acute{u}_j}$ as Reynolds stress and $-\rho\overline{\acute{T}\acute{u}_j}$ is used in relation to the turbulence to the temperature and mean velocity and illustrate the effect of turbulent and Boussinesq.

$$-\rho\overline{\acute{u}_i\acute{u}_j} = \mu_t\left(\frac{\partial u_i}{\partial x_j} + \frac{\partial u_j}{\partial x_i}\right) \text{ and } -\rho\overline{\acute{T}_i\acute{u}_j} = \frac{\mu}{Pr_t}\left(\frac{\partial T}{\partial x_j}\right) \tag{10}$$

Where the turbulent viscosity (μ_t) must be modeled, and the turbulent Prandtl number (Pr$_t$)

Turbulence model:

The modeled transport equations for k and ε in the realizable k-ε model are:

$$\frac{\partial(\rho k u_j)}{\partial x_j} = \frac{\partial}{\partial x_j}\left(\left(\mu + \frac{\mu_t}{\sigma_k}\right)\frac{\partial k}{\partial x_j}\right) + G_k + G_b - \rho\varepsilon - Y_M + S_k \tag{11}$$

$$\frac{\partial(\rho\varepsilon u_j)}{\partial x_j} = \frac{\partial}{\partial x_j}\left(\left(\mu + \frac{\mu_t}{\sigma_\epsilon}\right)\frac{\partial \varepsilon}{\partial x_j}\right) + \rho C_1 S\varepsilon - \rho C_2 \frac{\varepsilon^2}{k+\sqrt{\varepsilon v}} + C_{1\varepsilon}\frac{\varepsilon}{k}C_{3\epsilon}G_b + S_\varepsilon \tag{12}$$

where; $C_1 = \max\left[0.43, \frac{\eta}{\eta+5}\right], \eta = S\frac{k}{\varepsilon}, \ S = \sqrt{2S_{ij}S_{ij}}$

Boundary conditions for this study:

At inlet	U= v_{in}, v_x= 0, T =T_{in}	(13a)

At outlet $\quad \frac{\partial u}{\partial x} = 0, \frac{\partial u}{\partial y} = 0$, T= T_{out} (13b)

At the top and bottom walls: u = 0, v = 0 (13c)

At the tubes' surface u = 0, v = 0, T =T_s (13d)

The grid size affects the accuracy of the numerical solution and its necessity for fluid flow details, Figure 3 shows the meshed domain, resulted from ANSYS 20 that was applied to mesh the model with prescribed boundary conditions. Air as a working fluid with constant thermophysical properties was used. A two-dimensional computational domain that includes the air inlet, tube array, top and bottom walls, and pressure outlet. The working fluid, as a computational domain is meshed with quadrilateral and triangular mesh as a maximum element size of 0.02mm in the direction of the wall and the test portion, the mesh is quite fine including the arrays of tubes. The option of the inflation method is first thickness layer for meshing the tube surface, the transition ratio of 0.272, a growth ratio of 1.2, the initial height is 0.0002 m, were used, and the mesh quality of 0.65 resulted in a non-uniform mesh with no generation mesh of the material inside the tube. The following step is to choose the method where the pressure based steady-state becomes chosen, and the inlet and mass flow rate designed at realizable k- ε turbulent of a simple model.
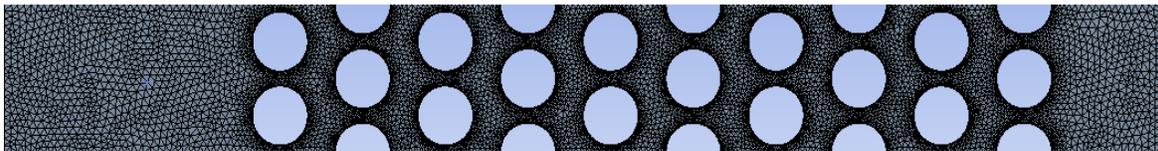
Fig.3: Computation domain

4. Results and discussions

4.1 Model validation

To check the validity and consistency of the present model its results are compared with those of Aiba et al. [14] and Zukauskas [15]. Figure 4 shows a high similarity between the results of the current model for the staggered tube bank pattern's average Nusselt number against Reynolds number and that of Aiba et al [14] and Zukauskas [15]. The average percentage deviation between the present model results and that of Aiba et al is about 8% and that of Zukauskas [15] is about 3%.
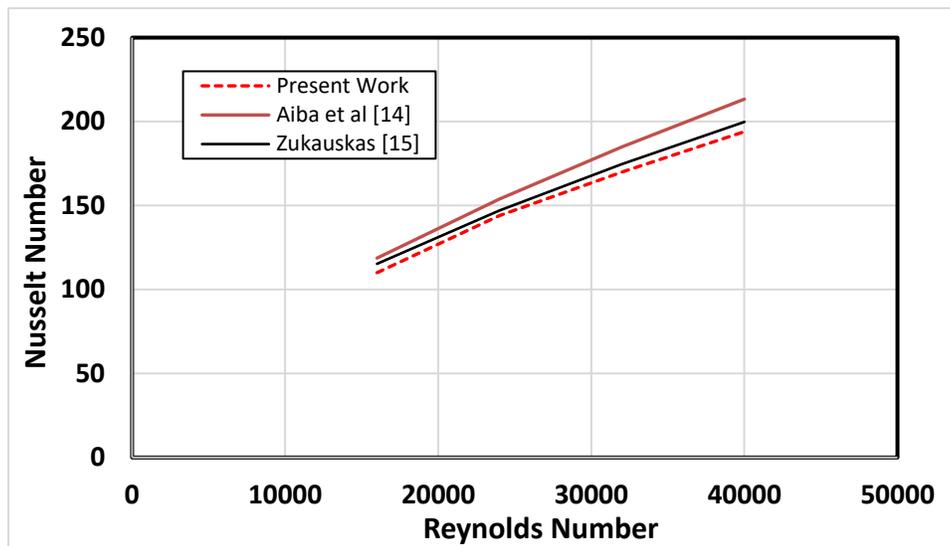
Fig.4: Effect of Reynolds number on average Nusselt number

4.2 CFD simulation

The current study is to illustrate the fluid behavior and the heat exchanging between the tube bank and the flowing fluid passing over. Different cases for different a number of tubes of 20, 30, 40, 50, 60, and 70 tubes with different rows, with tube diameter of 25 mm, and longitudinal and transverse pitch to tube diameter ratio of 1.5 and 1.25 respectively are investigated.

Figure 5 shows how the Reynolds number based on the maximum velocity affects the variation of the average Nusselt number on the surface of the tubes bank for both aligned and staggered 20-tubes bank pattern with 10 rows. The figure shows that when the Reynolds number increases the average Nusselt number increases and an average increase percentage of 14% for staggered design over the aligned pattern and this may be due to better mixing of air stream in the staggered pattern. This behavior reflected on variation of the pressure drop in Pa against Reynolds number illustrated in Fig. 6. As Reynolds number increases the pressure drop increases. The figure shows an average increase percentage of about 200% for the staggered pattern over the aligned one. Figure 7 shows

the variation of the temperature drop for the flowing air with Reynolds number. Also, the enhanced heat transfer for staggered pattern due to better air mixing leads to an average percentage increase of outlet temperature drop for the flowing air of about 61% over the aligned pattern. The temperature contours for the staggered pattern of 20-tubes with10 rows for Reynolds number of 16000, 24000, 32000, and 40000 respectively is shown in Fig. 8a-d. This figure confirms the result obtained from the Fig. 7, which is the higher the Reynolds number, the lower the temperature drop. This may be attributed to the lower residence time for air contact with the tube bundle at higher Reynolds number dimensioning the temperature drop of the flowing air. Also, higher temperature gradient is noticed at lower velocity due to the longtime of air passing over the surfaces of the tube bank and decreasing of wake formation. The temperature contours for the best Reynolds number (16000) for the aligned and staggered tube bank patterns is illustrated in Fig. 9a-b respectively. The figure demonstrates that in the aligned pattern the mixing of air and thus the uniformity of temperature at any plane perpendicular to the flow direction is low than that of the staggered pattern and thus it can be stated that the bypass factor for the aligned patterns is larger than that of the staggered pattern. The effect of Reynolds number on the static pressure distribution is demonstrated in Fig. 10a-d for Reynolds number values of 16000, 24000, 32000 and 40000 respectively. It noted that many computational runs for different values of rows and columns but for brevity the staggered tube bank of 2x10 is chosen for presentation. From the scale beside the figures, it is observed that the scale range increases with the increase of Reynold number that is mean as the Reynolds number increase the pressure drop of the air flowing across the tube bank increase and this result confirms that obtained from Fig. 6. Also, at any Reynolds number as the flow proceeds across the tube the pressure decreases with noticeable lower values of pressure between the tubes that agree with Bernoulli equation. Figure 11 demonstrates the pressure distribution by illustrating the static pressure contours at Re=16000 for both aligned and staggered 2x10 tube bank pattern respectively. A higher-pressure drop is noticed for staggered pattern that is agree with the result from Fig. 6 with lower values of pressure in narrow flow areas at any plane perpendicular to the flow direction.
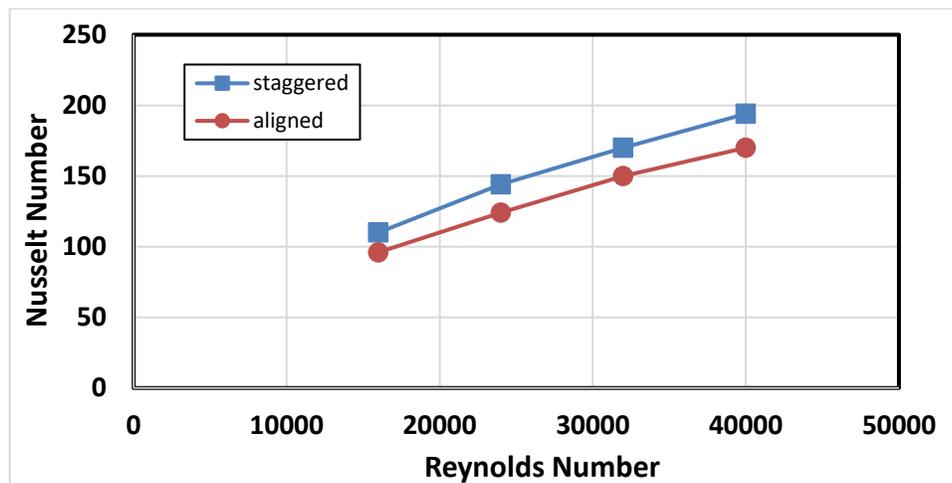

Fig. 5: Variation of Nusselt number with Reynolds number for aligned and staggered tube bank arrangement
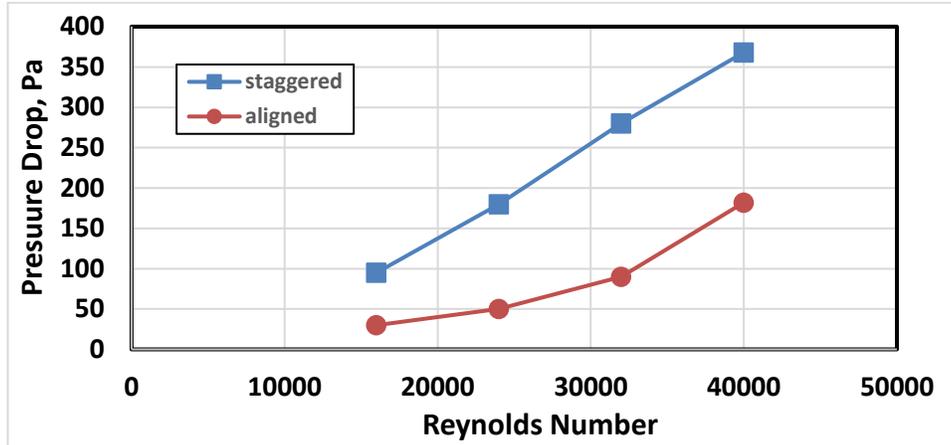
Fig. 6: Variation of Pressure drop with Reynolds number for aligned and staggered tube bank arrangement

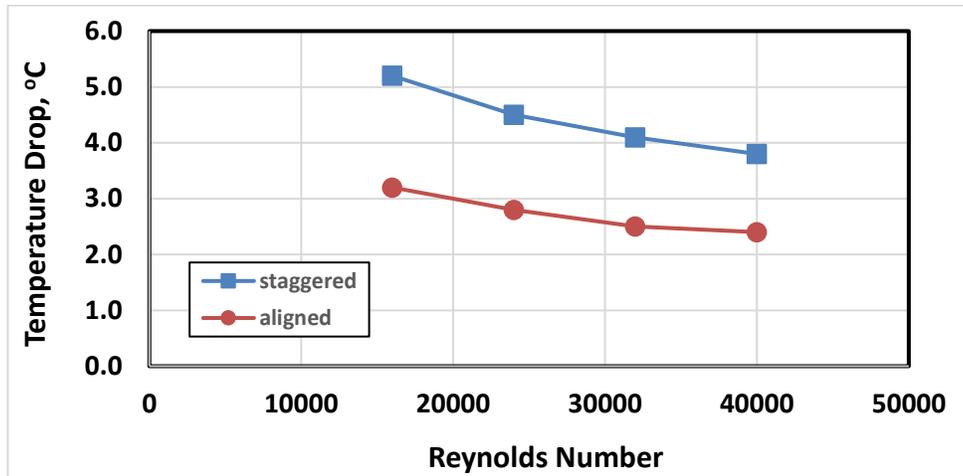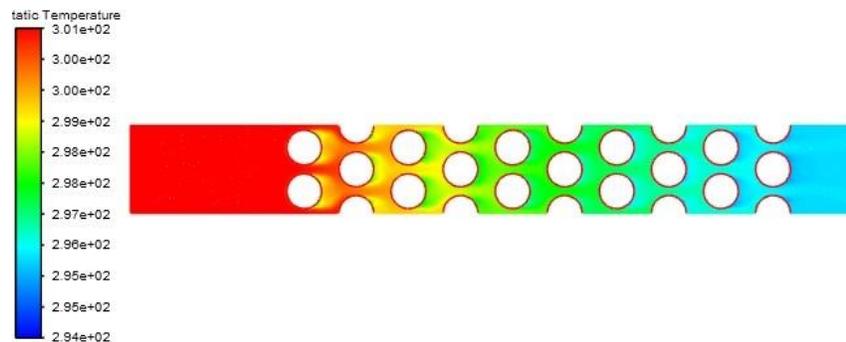**Fig. 7: Variation of air temperature drop with Reynolds number for aligned and staggered tube bank arrangement**
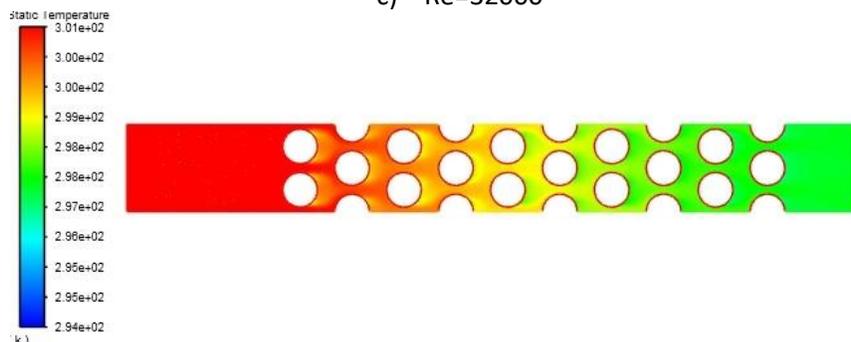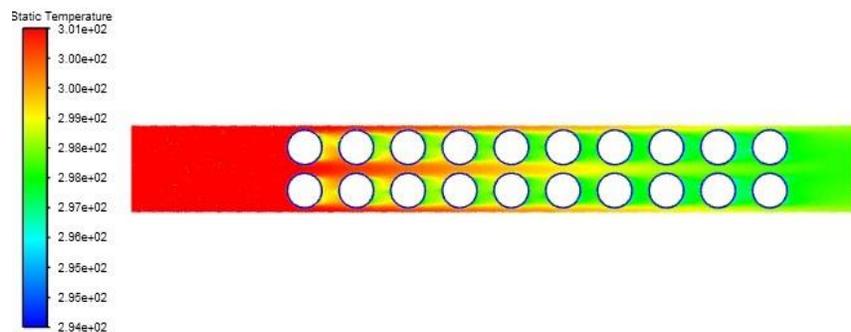

a)   Re=16000

b)   Re=24000

c)   Re=32000

d)   Re=40000

Fig. 8: Temperature contours for different Reynolds numbers for staggered pattern
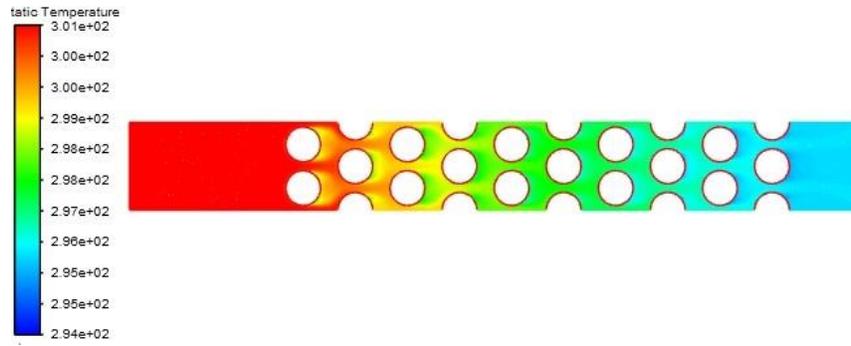
a)   aligned

b) Staggered
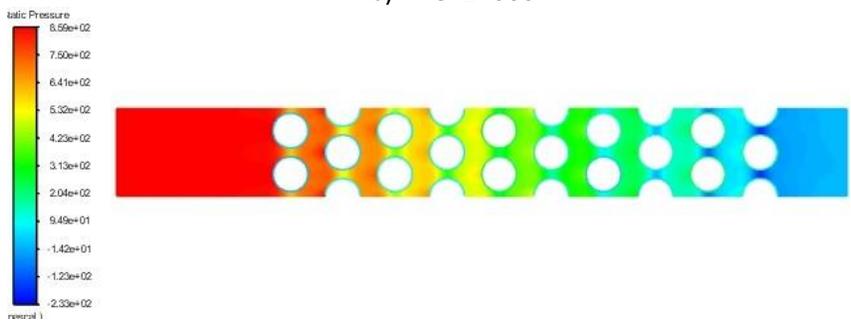
Fig. 9: Temperature contours at Re=16000 for a) aligned pattern and b) staggered pattern

a) Re=16000
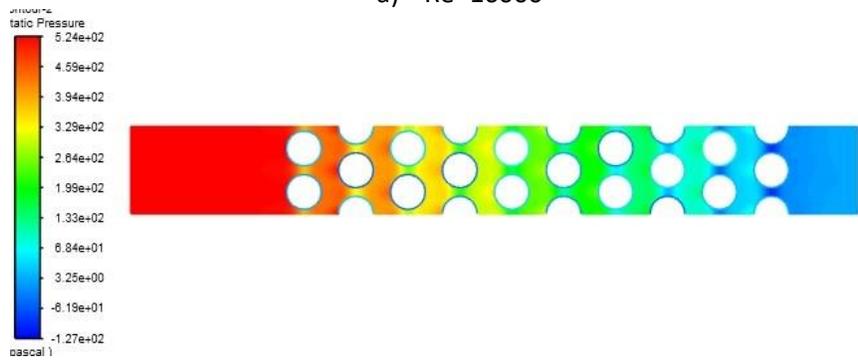
b) Re=24000
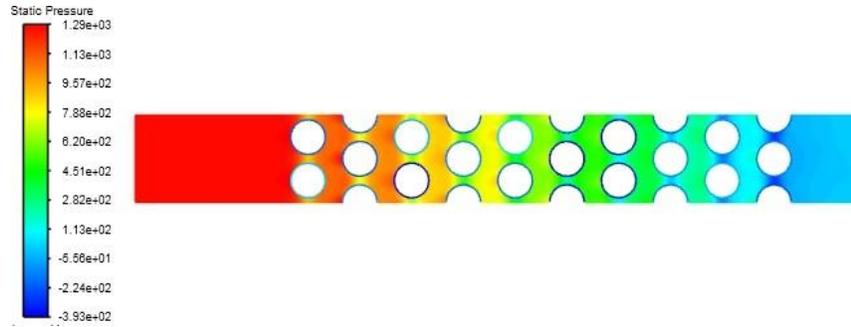

c) Re=32000
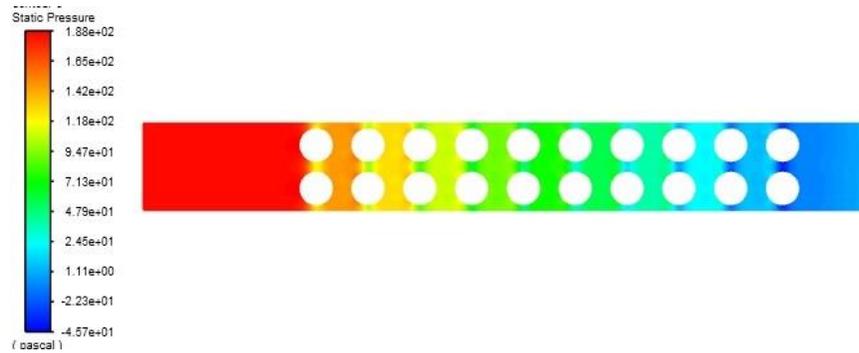
d) Re=40000

Fig. 10: Pressure contours for different Reynolds numbers for staggered pattern

a) aligned

b) staggered

Fig. 11: Pressure contours at Re=16000 for a) aligned pattern and b) staggered pattern

Figure 12 illustrate the variation of the average Nusselt number with the number of rows in the flow direction for staggered tube bank patterns. The figure shows an average percentage increase of Nusselt number ranges from 1.79% at Re=16000 up to 8.89% at Re=40000 for increasing the number of rows from 5 to 10. The effect of flow path length on pressure drop is depicted in Fig. 13. It is observed from the figure the as the number of rows increases the pressure drop increases with a percentage increase of about 76% at Re=16000, about 83% for Re=24000 and 32000 and about 41.5% at Re=40000 by increasing the number of rows from 5 to 10. The variation of temperature drops with the number of rows in the flow direction i.e., flow path length at different values of

Reynolds number is demonstrated in Fig. 14. It is observed from the figure that as the number of rows increases the temperature drop increases reaching asymptomatic value, it is recommended to compromise between the cost installation and thermal benefits.
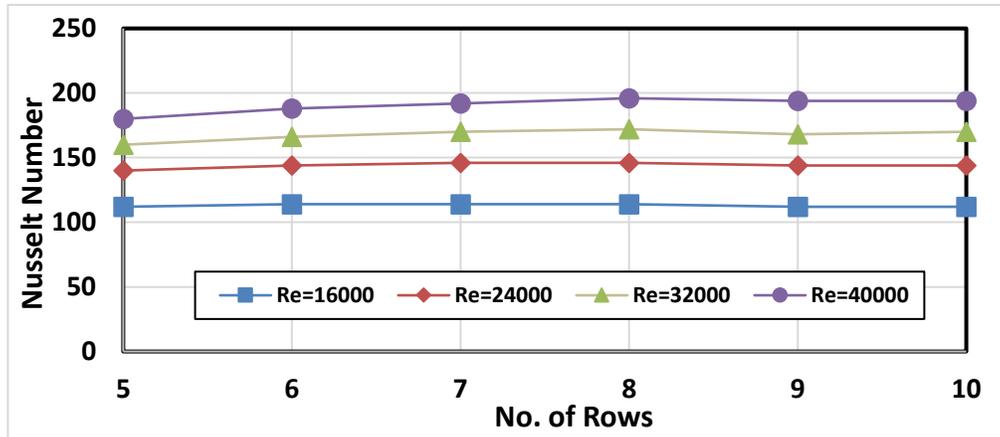

Fig. 12: Variation of Nusselt number with the number of rows in staggered pattern for different Reynolds numbers
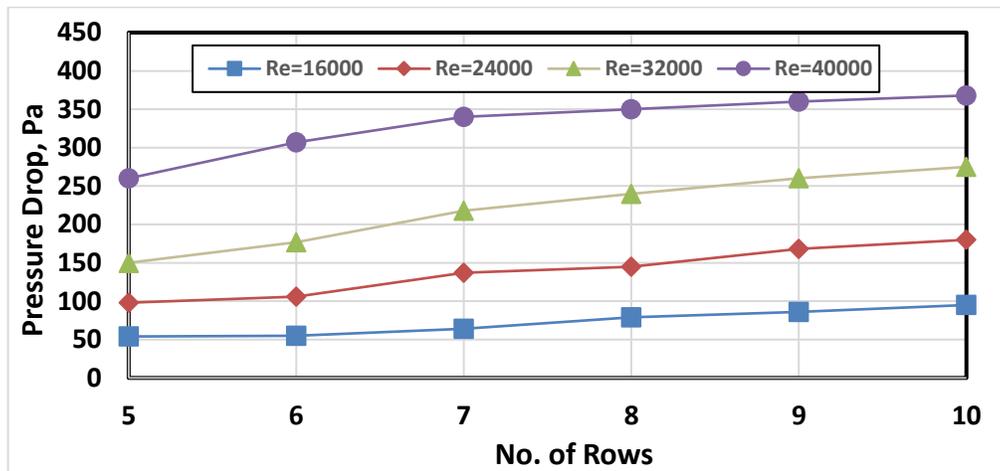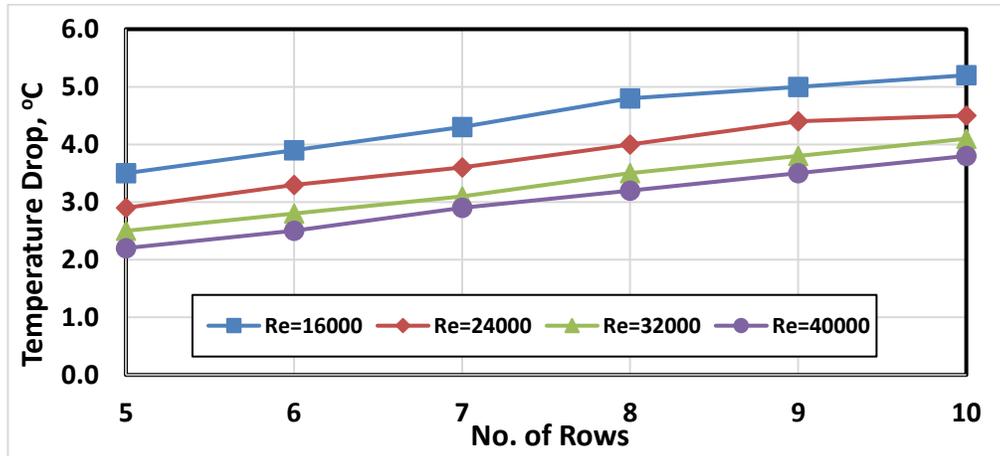

**Fig. 13: Variation of pressure drop with the number of rows in staggered pattern for different Reynolds numbers**

Fig. 14: Variation of outlet temperature with the number of rows in staggered pattern for different Reynolds numbers

4.3 Deduced Correlations

4.3.1 Average Nusselt number

The data presented in Fig. 5 is utilized to correlate the average Nusselt number with Reynolds number for aligned and staggered tube bank patterns as illustrated in Fig. 15a-b respectively

a) aligned   b) staggered
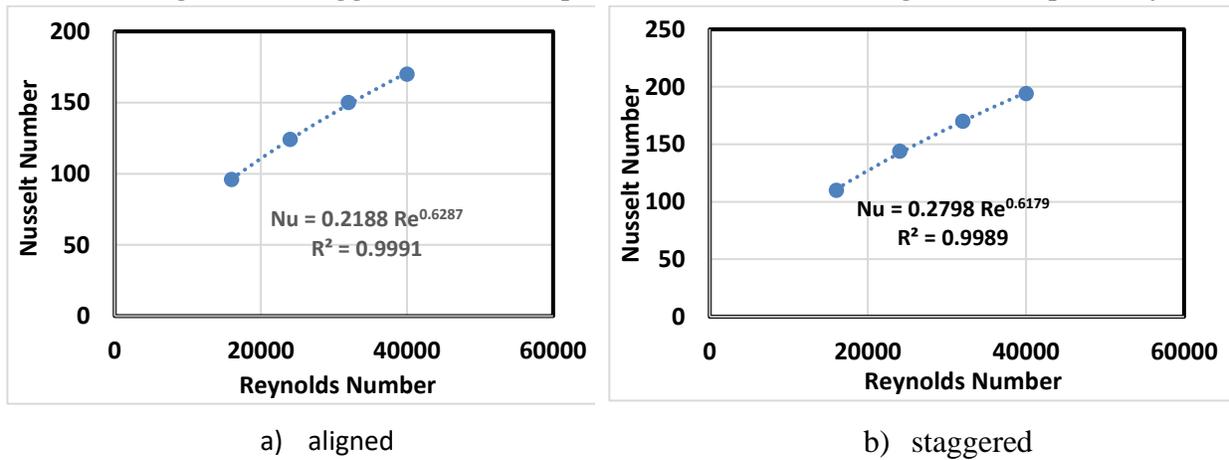
Fig. 15 Nusselt number vs Reynolds number correlation for aligned and staggered arrangement

$Nu=0.2188\,Re^{0.6287}$, for aligned pattern, $16000 \leq Re \leq 40000$ (14a)

$Nu=0.2798\,Re^{0.6179}$, for staggered pattern, $16000 \leq Re \leq 40000$ (14b)

Also, the average Nusselt number is correlated with both Reynolds number and the number of rows in the flow direction for staggered tube bank arrangement using the data shown in Fig. 12. This correlation is given as:

$Nu=0.419Re^{0.5677}N_L^{0.0528}$, for staggered pattern   (15a)

and $16000 \leq Re \leq 40000$ and $5 \leq N_L \leq 10$ and the correlation is depicted in Fig. 16 with average percentage error of $\pm 2\%$. For brevity only the correlation of aligned patterns is written as:

$Nu=0.195\ Re^{0.572}N_L{}^{0.318}$, for aligned pattern with error of $\pm 10\%$ (15b)
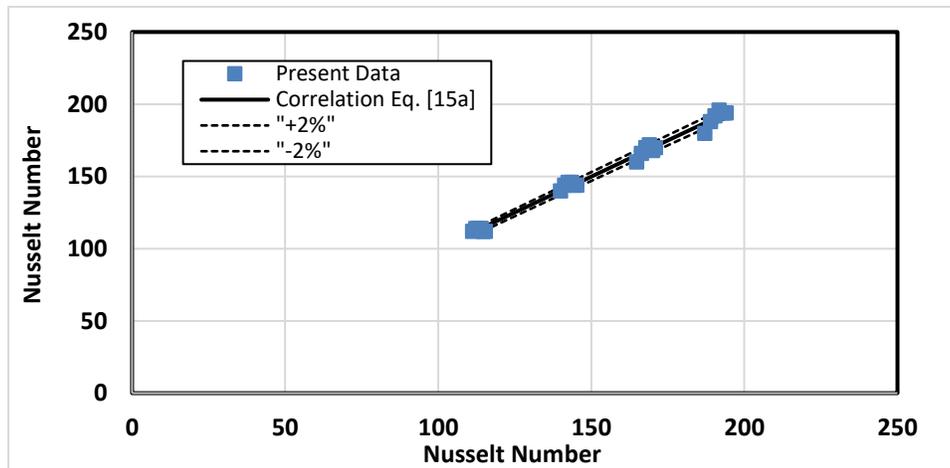
4.3.2 Air temperature drop percentage

The percentage of the temperature drop which is defined as the actual temperature drop to the maximum temperature drop for the air flowing over the tube bank is correlated in terms of Reynolds number as well as the number of rows of tubes in the flow direction as:

$$\theta = \frac{\Delta T_{act}}{\Delta T_{max}} = 1086.5Re^{-0.436}N_l^{0.694} \quad \% \text{ for staggered array}$$ (16a)

and the correlation is depicted in Fig. 17 with average percentage error of $\pm 3\%$. Also, for sake of brevity the correlation can be written as:
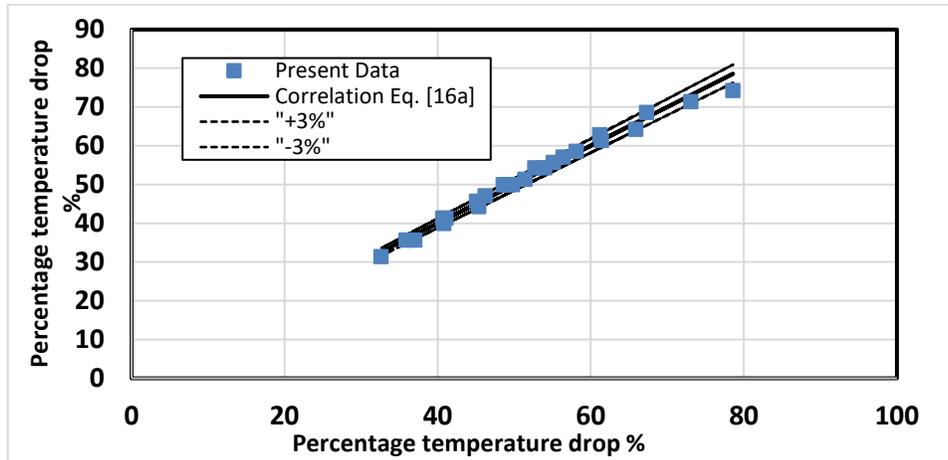
$$\theta = \frac{\Delta T_{act}}{\Delta T_{max}} = 601.68Re^{-0.396}N_l^{0.703} \quad \% \text{ for aligned array}$$ (16b)

The above two correlation are applied for $16000 \leq Re \leq 40000$ and $5 \leq N_L \leq 10$

Fig. 16 Nusselt number vs Reynolds number and number of rows correlation for staggered arrangement

Fig. 17 Percentage temperature drop vs Reynolds number and number of rows correlation for staggered arrangement

Figure 17 shows that the percentage temperature drop ranges between about 31% and 75% with average percentage of about 53%, as the maximum temperature drop equal to the difference between the inlet air temperature and sea water temperature which are assumed to be equal to 28°C and 21°C respectively, so the maximum and minimum temperature drops in the tube bank are 5.25°C and 2.17°C respectively.

A simple comparison between the air-conditioning system with seawater air precooling and the conventional system shows for the return air from an air-conditioned space is usually 24°C, when mixed with the outside fresh air it assumed to be 28°C for both systems, so the temperature difference between mixed air temperature and supply air temperature to the conditioned space is ΔT= 28 -14 = 14°C. This temperature drop takes place in both the air precooler and the evaporator cooling coil. So, when using air precooler with minimum and maximum temperature drop leads to minimum and maximum energy saving of 15.5% and 37.5% respectively.

Conclusions

The thermal performance of tubes and pressure drop with staggered and inline arrangements has been studied for 4 inlet velocities (Reynolds number) and different number of columns and rows with diameters of 25 mm, for longitudinal and transverse pitch ratios of the remarks are based on the numerical results of heat transfer

- The thermal performance for all cases increases with a decrease in airstream velocity for both inline and staggered arrangements, but more enhancement for staggered tube array relative to the inline flow because the main flow path is more torture and increased the mixing flow relative to the inline tube array.
- From the numerical predictions, it is found that the minimum and maximum energy saving lies between 15.5% and 37.5%. with using a staggering array tube.

- Useful correlations for the average Nusselt number and the percentage of water temperature drop across the staggered and aligned tube bank patterns are obtained.
- It is possible to use shallow water in cooling operations to save energy for partial air cooling in the air handling unit.

Nomenclature

A	surface area (m^2)	T	temperature (K or °C)
A_T	throat area (m^2)	u_i, u_j	velocity component (m/s)
A_D	diagonal area (m^2)	U	Free stream velocity of air (m/s)
D	tube diameter (m)	V	velocity of air (m/s)
f	friction factor (--)	x_j	coordinate in the j direction
h	heat transfer coefficient ($W/m^2\,K$)	**Greeks**	
K	thermal conductivity (W/m. K)	$\alpha_k, \alpha\varepsilon$	inverse of effective Prandtl number
k	turbulent kinetic energy	ε	dissipation of kinetic energy
N_L	number of rows (--)	Δ	difference
N_T	number of columns (--)	μ	dynamic viscosity (Pa.s)
Nu	average Nusselt number (--)	μ_t	turbulent viscosity (Pa.s)
p	Pressure (Pa)	ρ	density of air (kg/m^3)
Q	heat transfer rate (W)	**Subscripts**	
Re	Reynolds number	a	air
S_L	longitudinal pitch (mm)	s	Tube surface
S_T	transverse pitch (mm)	min	minimum
S_{ij}	mean strain rate tensor	max	maximum

References

[1] Lee, D., Ahn, J., Shin, S., 2013, "Uneven longitudinal pitch effect on tube bank heat transfer in cross flow", Applied Thermal Engineering 51 937-947

[2] Xu, J., Li, J., Ding, Y., Fu, Q., Cheng, M., Liao Q., 2018, "Numerical simulation of the flow and heat-transfer characteristics of an aligned external three-dimensional rectangular-finned tube bank", Applied Thermal Engineering 145 110–122

[3] Liu, M., Bescos, C. J., Calactin, J., 2022, "CFD investigation of a natural ventilation wind tower system with solid tube banks heat recovery for mild-cold climate", Journal of Building Engineering 45, 103570

[4] Souza, P. D., Biswas, D., and Deshmukh, S. P. 2020, "Air side performance of tube bank of an evaporator in a window air conditioner by CFD simulation with different circular tubes with uniform transverse pitch variation", International Journal of Thermofluids, J. homepage: www.elsevier.com/locate/ijtfhttps://doi.org/10.1016/j.ijft.2020.100028.

[5] Peláez R. B., Casanova J.O., López J.M.C., 2010 "A three–dimensional numerical study and comparison between the air side model and the air/water side model of a plain fin – and – tube heat exchanger" Applied Thermal Engineering 30, 1608-1615

[6] Medina, Y. C. Gonzales, Á.M. R.O., Fonticiella, M. C., Morales , O. F. G., Toledo, R. V., and Sardiñas, R. Q., 2018 "Simplified analysis of heat transfer through a finned tube bundle in air-

cooled condenser-second assessment", Mathematical Modelling of Engineering Problems, Vol. 5, No. 4, pp. 365-372 Journal homepage: http://iieta.org/Journals/MMEP

[7] Khan, W. A., Culham, J. R. and Yovanovich, M. M., 2007 "Optimal design of tube banks in crossflow using entropy generation minimization method", Journal of Thermophysics and Heat Transfer Vol. 21, No. 2.

[8] Sahamifar, S., Kowsary, F. , Mazlaghani, M. H., 2019, "Generalized optimization of cross-flow staggered tube banks using a subscale model", International Communications in Heat and Mass Transfer 105 46–57

 [9] Abdel-Rehim, Z. S., 2015, "Heat Transfer and Turbulent Fluid Flow Over Staggered Circular Tube Bank" ISSN: 1556-7036 print/1556-7230 online, DOI: 10.1080/15567036.2011.582609 Energy Sources, Part A: Recovery, Utilization, and Environmental Effects, 37:164–173.

[10] Mangrulkar, C. K., Dhoble, A S., and Chakrabarty, S G., Wankhede, U S., 2016 "Experimental and CFD prediction of heat transfer and friction factor characteristics in cross flow tube bank with integral splitter plate" www.elsevier.com/locate/ijhmt DOI: 10.7763/IJCEA.2013.V4.330

[11] Elmekawy, A. M. N , Ibrahim, A. A., Shahin, A. M, Al-Ali, S., Hassan, G. E., 2021, "Performance enhancement for tube bank staggered configuration heat exchanger – CFD Study" , Chemical Engineering & Processing: Process Intensification 164 108392.

[12] Abraham, J. D., Dhoble, A. S., and Mangrulkar, C. K., 2020, "Numerical analysis for thermo-hydraulic performance of staggered cross flow tube bank with longitudinal tapered fins", International Communications in Heat and Mass Transfer 118, 104905

[13] Surroop, D. and Abhishekanand, A., 2013 "Technical and Economic Assessment of Seawater Air Conditioning in Hotels," Int. J. Chem. Eng. Appl., vol. 4, no. 6, pp. 382–387.

[14] Aiba, S. Tsuchida, H. Ota, T., 1982, "Heat transfer around tubes in staggered tube banks", B. JSME 25 (204) 927–933.

[15] Zukauskas, A., 1972, "Heat Transfer from Tubes in Cross Flow," in J. P. Hartnett and T. F. Irvine, Jr., Eds., Advances in Heat Transfer, Vol. 8, Academic Press, New York.

[16] Etaiwe, H.A. Sakr, R.Y. Salem, M. R. Abdelrahman, H.E., 2022, "Solar Driven Absorption Air Conditioning System Using Seawater for Air Precooling", Journal of Al-Azhar University Engineering Sector (JAUES)- under publication.